Journal of Textiles and Polymers

Vol. 12, No. 1, 43-52, March 2024
https://www.itast.ir
DOI: 10.48302/jtp.2025.528342.1315

Effects of fibrous layer structure on tensile behavior and fracture toughness of e-glass/epoxy composites: a comparison between angle plied and woven layers

Azam Alirezazadeh[1], Sayyed Mahdi Hejazi[1*], Ali Zadhoush[1] and Saleh Akbarzadeh[2]

[1] Department of Textile Engineering, Isfahan University of Technology, Isfahan, 84156-83111, Iran.
[2] Department of Mechanical Engineering, Isfahan University of Technology, Isfahan, 84156-83111, Iran.

Article Information

Article history:

Received: 2025-10-30

Accepted: 2025-11-15

***Keywords*:**

Fracture toughness, fibrous layer structure, tensile properties, epoxy composite, E-glass fiber.

Abstract

The fibrous layer structure plays a pivotal role in determining the mechanical performance of fiber reinforced polymer composites (FRPCs). Studying the influence of fibrous layer structure on fracture behavior of FRPCs, as one of the key mechanical characteristics, is crucial to improve safety and complex load bearing capacity of advanced structures. Therefore, the main objective of this research is to compare the tensile behavior and crack growth in two types of E-glass/epoxy composites and to examine how the structure of fibrous layers influences the mechanical properties of the composite. Samples were produced in a four-layer configuration using vacuum infusion process (VIP). The first sample consisted of four layers of woven fabric arranged at ±45°, while the second sample was made from four angle plied layers with a fiber orientation of ±45°. Before conducting tensile and fracture tests, microbond tests were performed to explore any possible differences between the fiber/matrix interfacial properties within the two composite samples. Physical characteristics including thickness, density, fiber volume fraction and void content in the two composite samples were also evaluated. Then, the composite samples were subjected to tensile tests. To investigate mode I fracture toughness, the samples were single-edge notched and then subjected to tensile tests. Results indicated that the composite reinforced with woven layers exhibited high tensile strength and stiffness but was more sensitive to crack growth. The composite with angle plied layers, despite being thicker, showed 28.47% higher stress intensity factor and 56.63% higher critical energy release rate, compared with the woven counterpart.

1 INTRODUCTION

Fiber-reinforced polymer composites (FRPCs) are widely used in various industries, including aerospace, automotive, and construction, due to their high strength-to-weight ratio, corrosion resistance, and design flexibility [1]. The mechanical performance of FRPCs is influenced by several factors, including fiber type, manufacturing technique, fiber orientation/arrangement, and matrix properties [2]. One critical mechanical property determining the structural integrity of composites is fracture toughness, which measures the resistance of the material to crack propagation. Enhancing the fracture toughness of composites is essential for improving their durability in various applications [3]. Depending on the type of application, the mechanical properties of the FRPCs are designed and engineered to meet specific requirements. For instance, the fracture toughness values in FRPCs used for construction and building materials are significantly lower than those used in aerospace applications. The type of fibers and resin used in each application varies. Among the wide range of materials used in this field, epoxy composites reinforced with E-glass fibers are particularly popular due to their cost-effectiveness and suitable mechanical properties [4]. However, the arrangement and positioning of the fibers within the composite structure can significantly influence the properties of the composite, including the fracture toughness.

In various studies, the effects of specific structural parameters of composites on different mechanical properties have been investigated. It has been shown that the effects can vary depending on the arrangement of the fibers and the type of structure. For instance, considering the orientation of fibers and yarns, Nayak et al. [5] investigated the mechanical properties of 3D E-glass reinforced epoxy composites. It was found that the composites with 0° binder yarn orientation showed the highest mechanical properties, compared to those having binder yarns in 30, 45 and 60° orientations. In another work conducted by Raghavendra et al. [6], the effects of bi-directional (all layers at 0° and 90°) and multi-directional (laid at 0°, 15°, 30°, 45°, 60°, 75°, and 90°) woven glass fibers on the mechanical properties of epoxy composites were investigated. Results of the study showed that the maximum tensile and flexural strengths belonged to the composites reinforced by 12 layers of bi-directional fibers. Khatkar et al.

* Corresponding authors: hejazi110@iut.ac.ir

[7] studied the role of fiber reinforcement architecture in the mechanical performance of glass-fiber-reinforced epoxy composite materials. The unidirectional fibers provided excellent properties along the fiber direction, while the 3D architectures showed excellent properties (especially delamination and impact resistance) in all three directions. In another study by Bilisik et al. [8], the effects of linear density of yarns and areal density of fabrics on the bending behavior of multilayered multi-stitched E-Glass preforms were discussed. In a recent study by Risteska et al. [9], the impact of textile structure reinforcement including woven (plain, twill, basket), nonwoven mat, and unidirectional E-glass fibers on the flexural properties of epoxy composites was investigated.

Extensive research has been performed on studying the influence of textile structural parameters on the mechanical properties of glass fiber reinforced epoxy composites. However, the majority of the studies have focused on common mechanical properties including tensile, compressive, shear, bending, and impact behavior [10], while the fracture properties of the composites have been comparatively less analyzed. In recent years, numerous studies have investigated the fracture behavior of textile-reinforced composites. These studies have primarily focused on examining the influence of fibrous layers architecture and arrangement on toughening mechanisms and energy absorption [11, 12]. For instance, Sharma et al. [13] have explored the interlaminar fracture toughness of plain/twill woven carbon and Kevlar reinforced composites, as well as the effects of inter-yarn hybridization in textile composites. Tewani et al. [14] studied the role of weave sub-patterns on the mechanics of crack propagation in textile composites. The findings of these studies indicate that an appropriate design of fiber architecture can lead to significant improvements in fracture properties, enhanced toughness, and increased structural stability. Among the numerous studies in fracture behavior of FRPCs, most research works have focused on unidirectional structures; subsequently, more complex geometries have been simulated through modeling [15]. In this context, composites with angle plied fibrous layers have gathered significant attention for their ability to balance tensile and shear properties. Angle plied fibrous layer refers to the arrangement of fibers at specific angles relative to the primary axis of the material, with a stitching thread providing the necessary cohesion between the two layers [16]. In addition to angle plied layers, woven fabrics are also extensively utilized in composites [17]. The woven fabrics achieve sufficient cohesion through the weaving of the fiber bundles. To better understand the impact of fibrous layer structure on the mechanical properties of composites, comparing fracture behavior with changes in textile parameters, such as the type of fibrous layer arrangement, is crucial. This aspect has been less explored in the literature. Despite the extensive investigations on the overall mechanical properties, a systematic review of recent studies reveals that few comparative analyses have simultaneously examined the effects of laminate structure (woven vs. angle-ply) and geometrical factors (such as composite thickness) under fracture conditions. Therefore, an experimental study that compares these parameters under identical conditions (i.e., material type, areal density of layers, and interfacial properties) is essential to address this research gap.

Therefore, this study aims to investigate the tensile behavior and fracture toughness of two types of epoxy composites reinforced with glass fibers with the same material and areal density but with two different structures. The first sample consists of four layers of woven E-glass fabric arranged at ±45°, while the second sample is made from four layers of the same material with an equal areal density (400 $g.m^{-2}$) but constructed with angle plied layers at the same ±45° orientation relative to the applied load. To assess fracture toughness, the critical crack length a_C, critical stress intensity factor K_{IC}, and critical energy release rate G_{IC} (energy required to create a crack) were measured. The findings of this research will contribute to a better understanding of the impact of fibrous layer structure on the mechanical properties of composites, a topic that has received limited attention in previous studies.

2 METHODOLOGY

2-1 Materials

Bisphenol-A epoxy resin (EP411) and amine based hardener (H3) were provided from DSM Co. (Netherlands). E-glass fibrous layers with an areal density of 400 g.m-2, fiber diameter of 15 μm, and 1200 fibers per roving, were purchased from Sina Delijan Co. (Iran) and Changzhou Co. (China), featuring two different structures (as shown in Fig. 1a and b): woven fabric and angle plied layers, respectively.

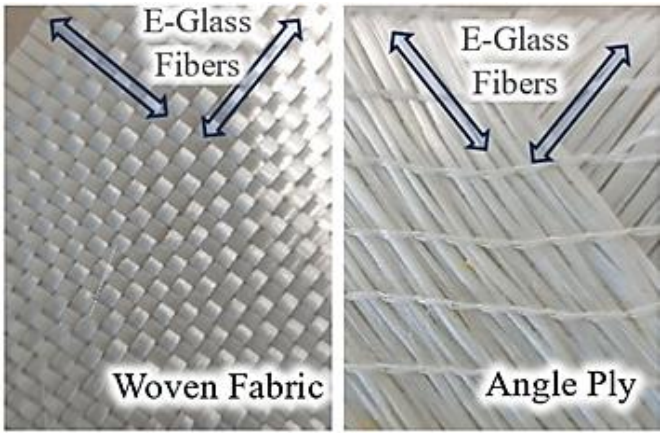

Fig. 1 E-glass fibrous layers in a) woven E-glass fabric and b) angle plied E-glass layer

2-2 Microbond test

The E-glass fibrous layers were both impregnated with a type of silane-based sizing, and no information was available about the uniformity, amount, and type of sizing in the two fibrous layers structures. Therefore, a microbond test was also performed to compare the mechanical properties at the interface between the fibers and the matrix, which could be affected by the sizing. This test was conducted to determine whether any differences in tensile behavior and fracture resistance between the two kinds of composites were attributable to the structural type of the fibrous layers, the type of sizing used (which influences the interfacial properties), or both. For sample preparation, individual E-glass fibers were carefully extracted from the fibrous layers under a large magnifying glass equipped with a lamp. Approximately 200 paper frames, specifically designed for the microbond test, were prepared (Fig. 2). Each frame had a hole to engage with

a metal hook, facilitating easier attachment of the samples to the machine's jaw and preventing premature rupture of the fibers. Each fiber strand was placed vertically in the paper frame using liquid cyanoacrylate adhesive, ensuring that the fiber could not easily detach from the frame. An oval droplet of a homogeneous mixture of resin and hardener (in a weight ratio of 100:5) was then placed on the middle of each fiber using a sharp needle. The length of the impregnation and the diameter of the droplets varied according to the amount of resin applied to each fiber. The impregnation length should not exceed a critical value to prevent the fiber from rupture before being pulled-out. It is assumed that the resin droplet maintains its geometry during curing, since the rapid increase in viscosity and surface tension at the fiber/resin interface restrict any noticeable change in droplet shape or contact area.

Fig. 2 Schematic illustration of the microbond test

According to the previous research studies, for fibers with diameters ranging from 5 to 50 μm, the impregnated length (l_i) must be between 50 and 1000 μm [18]. After completing the resin curing process (12 hours at room temperature and 3 hours at 80ºC), the fiber diameter, droplet diameter, and impregnation length were determined and recorded using an optical microscope. To conduct the microbond test, a highly precise testing machine (Zwick tester, model 144660) equipped with a 20 N load cell and a custom-made jaw for holding the microbond specimens was used. The lower jaw included a small caliper, where two moving caliper grips were positioned horizontally on a flat base to hold a single resin droplet, and a metal hook was attached vertically to the upper jaw to pull the fiber out of the droplet. The upper jaw displacement rate was set at 0.5 mm.min^{-1}, and the gage length was 200 mm.

According to the illustrations provided by Miller et al. [19], three possible scenarios may occur during microbond test: 1) droplet slippage, i.e., slippage of a microdroplet between the two grips (herein, caliper grips), 2) fiber break, i.e., fiber rupture prior to droplet detachment from the fiber surface, and 3) shear debonding, i.e., separation of the bond between the fiber and the droplet without fiber rupture. One of the main challenges in performing the microbond test is the high rate of fiber rupture before the microdroplet detachment. By selecting an appropriate fiber length and reducing the droplet size, the high rate of fiber rupture can be decreased. However, the deviations in test results remain high. Therefore, from a total of 100 tests from each fibrous layer, those with rupture occurring in areas other than the droplet-resin interface were excluded from the test results. Therefore, the results of at least 30 observations from each sample (presented as load-displacement curves) were considered to be the outcomes of the microbond test.

The maximum load from each microbond test was considered for the calculation of the apparent interfacial shear strength (τ_{app}) using Eq. (1) [20]:

$$\tau_{app} = \frac{F_{max}}{\pi d_f l_i} \quad (1)$$

Where, d_f is the fiber diameter, and l_i is the impregnated length. Since τ_{app} strongly depends on the droplet size, local property in the form of ultimate interfacial shear strength (τ_{ult}) is considered instead. Regarding the shear lag parameter $\beta = \left[8G_m/\left(E_f d_f^2 \ln(2\,r_m/d_f)\right)\right]^{0.5}$ in which $G_m = E_m/2(1+\nu_m)$ stands for the shear modulus of polymer matrix, E_f is the elastic modulus of fiber (herein, 72 GPa), r_m is the droplet radius, E_m is the elastic modulus of polymer matrix (herein, 2.36 GPa), and ν_m is the Poisson ratio of polymer matrix (herein, 0.35), τ_{ult} can be determined by Eq. (2) [20].

$$\tau_{ult} = \frac{dF}{\pi d_f l_i} = \frac{\tau_{app} l_i \beta}{tanh(l_i \beta)} + E_f \frac{d_f}{4} \beta(\alpha_f - \alpha_m)\Delta T tanh(\frac{l_i \beta}{2}) \quad (2)$$

Where, α_f is the thermal expansion coefficient of fiber (herein, α_f = 5.5 × 10^{-6} K^{-1}), and α_m is the thermal expansion coefficient of matrix (herein, α_m= 70 × 10^{-6} K^{-1}), and ΔT is the temperature change between ambient and curing condition of epoxy. Therefore, ultimate interfacial shear stress (σ_{ult}) can be obtained by $\sigma_{ult} = \tau_{ult}\sqrt{E_f/E_m}$. Work of adhesion ($W_A$) as one of the criteria for interfacial failure can also be calculated by Eq (13) [20]:

$$W_A \cong \frac{1}{2 \times 10^9} \times \tau_{ult} \sqrt{\frac{E_m}{E_f}} \quad (3)$$

2-3 Composite preparation

The composite was fabricated using a vacuum infusion process (VIP). For this purpose, a release wax was applied on the surface of a flat mold (tempered glass with a thickness of 7 mm). Then, a resin-injection mesh, a layer of peel-ply, four fibrous layers arranged at an angle of ±45º as composite reinforcement (Fig. 3 (a)), another layer of peel-ply, and an additional injection mesh were placed onto the flat mold. A sealing tape was then affixed around the working area, about 1 cm away from the edges. Two pieces of resin transfer tubes were also placed at the top and bottom of the working area to serve as resin extraction and injection tubes, respectively. A thin layer of vacuum bagging was placed over the sealing tape (excluding the resin injection and extraction tubes). A resin and hardener mixture was injected into a vacuum bag at a weight ratio of 100:15 (according to the manufacturer's specifications), as shown in Fig. 3 (b). The process continued until the entire surface of the fibrous layers was thoroughly saturated with resin and all visible bubbles were evacuated through the vacuum pump. Afterward, the resin injection and extraction tubes were sealed, and the system was left for 12 hours at room temperature to complete the first curing stage. The composite sheet was then removed from the assembly and placed in an oven at 80ºC to finalize the curing process

(according to the curing schedule provided in the manufacturer's datasheet).

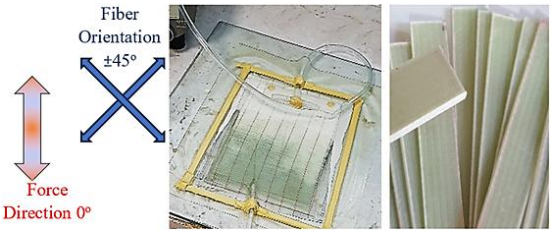

Fig. 3 a) fiber orientation and loading direction, b) resin injection in VIP method, c) sample cut to ASTM D3039 standard dimensions

2-4 Physical and Mechanical Properties of The Composites

The thickness of the samples was measured at three different points using a digital thickness gauge with an accuracy of 0.01 µm. The experimental density of the samples was determined using the Archimedes principle (ASTM D792), which involved submerging the composite samples in water. The difference between the experimental and theoretical density was used to calculate the void content. Subsequently, a burning test was conducted according to ASTM D3171 standard, where a specific amount of each sample was placed in a porcelain crucible and heated in an electrical furnace to 600ºC for 3 hours to remove the resin, leaving the glass fibers. By weighing the remaining fibers, the weight fraction and volume fraction of the fibers were calculated.

Following ASTM D3039 standard for the tensile properties of polymer composites, the resulting composite sheet was cut into pieces measuring 250 × 25 mm2 (Fig. 3 (c)) using a CNC machine. In total, five unnotched samples were prepared for tensile analysis and three notched samples for fracture assessment from each type of fibrous layer. According to ASTM D5045-99 standard for determining fracture parameters, a narrow notch with a thickness of 200 µm was created using an ultra-thin saw and a razor blade, extending halfway across the width of the samples. All samples were subjected to tensile tests at a constant elongation rate of 10 mm.min-1.

To determine K_{IC}, equation (1) was used [21]:

$$K_{IC} = \left(\frac{P_Q}{BW^{1/2}}\right) f(x) \quad (4)$$

Where, P_Q is the force at 1.05 times of the linear compliance of the force-displacement curve, B is the sample thickness, W is the sample width, and $f(x)$ is a function dependent on the sample geometry, which is obtained using the ratio of the notch width to the sample width (x) from equation (2) [21]:

$$f(x) = \frac{(2+x)(0.886 + 4.64x - 13.32x^2 + 14.72x^3 - 5.6x^4)}{(1-x)^{3/2}} \quad (5)$$

The parameter G_{IC} was obtained by integrating the area under the force-displacement curve, and the accuracy of the results was evaluated by equation (3) [21]:

$$G_{IC} = (1-\nu^2)K_{IC}^2/E \quad (6)$$

Where, ν, the Poisson's ratio, and E, the elastic modulus of the samples, were determined from tensile tests [21].

To determine a_C, the position of the crack tip was examined using image processing. Therefore, the real-time images of crack growth were processed using batch macro coding in ImageJ software (version 1.53t). The purpose of the image processing was simply to distinguish and identify the damaged zones from the normal regions. The image processing steps included split channels (blue), threshold (Huang), close/open/3D median filters (size 2 × 2 × 2) and image subtract.

Statistical analyses were also performed using IBM SPSS Statistics software (version 22) at a 95% confidence interval to compare the mean values of tensile strength, tensile modulus, strain at break, as well as the mean values of a_C, G_{IC}, and K_{IC}. As a final step, scanning electron microscopy (SEM) (Philips XL 30 LEO 1430VP-Carl Zeiss & Tescan Vega-3 LMU) was also employed to identify the microstructural failure mechanisms of the composite samples.

3 RESULTS AND DISCUSSIONS

3-1 Microbond Test Results

The variation in the type of sizing applied to the surface of E-glass fibers directly affects the adhesion and mechanical interlocking at the interface between the fiber and the polymer. Since the type and amount of sizing applied to the fiber surfaces in different fibrous layers were unknown, the droplet test was employed to compare the interfacial properties in two composite samples reinforced with angle plied fibrous layers and woven fabrics. The results of optical microscopy evaluation of the resin microdroplets on the E-glass fibers and interfacial properties from microbond tests are presented in Table 1. Despite the differences in the interfacial properties between fibers and matrices that can be observed in Fig. 4, analyses on standard deviations denote no significant differences between the interface properties of the two samples. Therefore, further discussions mainly relied on the structural characteristics of the two fibrous layers (woven fabric vs. angle plied layer) in epoxy composites.

Table 1 Results of optical microscopy evaluation of the resin microdroplets on the E-glass fibers and interfacial properties from microbond tests

Sample Code	Fiber diameter (d_f) (µm)	Microdroplets radius (r_m) (µm)	Impregnated length (l_i) (µm)	Apparent interfacial shear strength (τ_{app}) (MPa)	Interfacial shear strength (τ_{ult}) (MPa)	Work of adhesion criteria (W_A) (mJ.m^{-2})	Adhesion pressure (σ_{ult}) (MPa)
Angle Ply	15.8 ± 2.1	224 ± 170	512 ± 210	15.3 ± 3.2	127.9 ± 13.3	11.6 ± 0.1	706.5 ± 67.5
Woven	14.8 ± 1.1	210 ± 127	478 ± 198	16.2 ± 2.1	132.3 ± 19.0	11.9 ± 0.2	730.8 ± 72.3

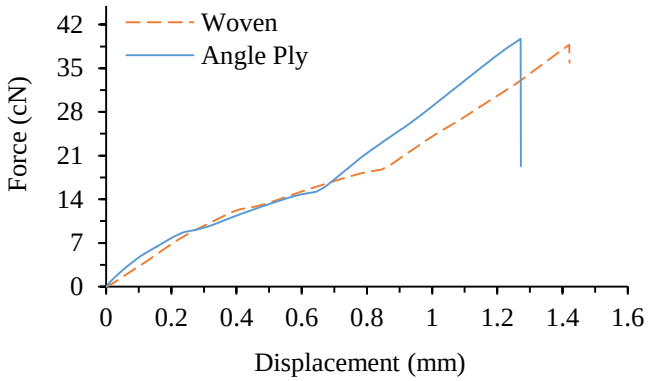

Fig. 4 Comparison between the force-displacement curves obtained from microbond tests on individual fibers of the two fibrous layers (woven fabric vs. angle plied layer)

3-2 Physical Properties of the E-glass/epoxy Composites

The thickness of the composite reinforced with woven layers (1.5 ± 0.1 mm) was found to be less than that of the composite reinforced with angle plied layers (3.33 ± 0.2 mm). It should be noted that each ply in angle-plied layers consisted of two layers that were stitched together to provide sufficient cohesion for the fibers. Therefore, the difference between the thicknesses of the two composite structures was logical. Theoretically, the densities of the two samples should be the same due to the equal areal densities of the fibrous layers; however, in fact, the density of the FRPC having woven fabric was found to be higher (Table 2). Given the constant areal density of the layer (400 g.m-2), it can be concluded that the woven structure provides greater cohesion to adjacent fibers in the composite structure. This may lead to improved composite strength due to better fiber cohesion and a more uniform stress distribution.

Table 2 Thickness, density, fiber volume fraction, and void contents in the epoxy composite samples reinforced with E-glass woven fabrics and angle-plied layers

Sample	Woven Fabric	Angle Ply
Thickness (mm)	1.5 ± 0.1	3.33 ± 0.2
Experimental Density (g.cm^{-3})	1.96 ± 0.01	1.94 ± 0.01
Theoretical Density (g.cm^{-3})	2.01	2.01
Void Content (%)	2.49 ± 0.1	2.98 ± 0.1
Fiber Volume Fraction (%)	51.53 ± 0.5	50.50 ± 0.5

The difference in void content between the two composite samples appears relatively minor at first sight (2.49% vs. 2.98%). However, it actually represents a relative variation of about 19.68%, which can affect the mechanical behavior of the composite. Voids locally induce stress concentrations and promote the initiation of microcracks within the matrix under tensile stress. Therefore, the effective load-bearing capacity of the composite in a reduced cross-sectional area decreases, leading to premature composite failure. Furthermore, if the voids are sufficiently large and located at the fiber/matrix interface, they can reduce the actual contact area between the fiber and matrix. Hence, even a slightly higher void content in the angle-plied composite may contribute to a partial degradation of tensile properties. Nevertheless, a limited amount of small voids within the epoxy matrix can facilitate localized plastic deformation around the voids and promote energy absorption near crack tips.

3-3 Tensile Behavior and Fracture Toughness of the E-glass/epoxy Composites

According to the analysis of variance (ANOVA) test, as presented in Table 3, significant differences were observed between the means of tensile properties and fracture toughness parameters (all p-values were less than 0.05).

Table 3 The results of statistical analyses for comparing the mean values of tensile properties and fracture toughness parameters in woven and angle-plied composites

		Sum of Squares	df	Mean Square	F	Sig.
Tensile Strength	Between Groups	209.581	1	209.581	9.885	0.014
	Within Groups	169.609	8	21.201		
	Total	379.190	9			
Maximum Strain	Between Groups	178.422	1	178.422	26.054	0.001
	Within Groups	54.785	8	6.848		
	Total	233.206	9			
Elastic Modulus	Between Groups	446.037	1	446.037	817.220	0.000
	Within Groups	4.366	8	0.546		
	Total	450.403	9			
K_{IC}	Between Groups	1072.541	1	1072.541	11.577	0.027
	Within Groups	370.587	4	92.647		
	Total	1443.128	5			
G_{IC}	Between Groups	11.289	1	11.289	13.330	0.022
	Within Groups	3.387	4	0.847		
	Total	14.676	5			
a_C	Between Groups	1.782	1	1.782	8.466	0.044
	Within Groups	0.842	4	0.211		
	Total	2.624	5			

According to Fig. 5 (a), the higher tensile strength and modulus of the composite reinforced with woven fabrics indicate that the sample containing the woven fabric has a stiffer nature and can withstand higher loads. This result suggests greater efficiency of the fibers and the intertwined nature of the weave. However, the lower strain in this type of composite indicates catastrophic failure. This behavior correlates with K_{IC} (Fig. 6 (a)) and has a direct relationship with the critical force in the force-displacement curve of the notched sample (Fig. 5 (b)).

Lower values of K_{IC} in the composite reinforced with woven fabrics (Fig. 6 (a)) denote its sensitivity to crack propagation. This result can be attributed to the nature of the weave, which, although strong, may not effectively dissipate energy when a crack initiates. Higher values of G_{IC} and a_C in the composite reinforced with angled layers (Fig. 6 (b) and (c)) suggest that this sample can absorb more energy before failure, indicating better performance of the angled layers under conditions that promote crack growth. In the fracture test, greater elongation and lower force in the composite reinforced with woven fabrics indicate that this composite does not have high resistance to crack propagation and is more sensitive to defects.

Fig. 7 shows the crack growth in two different samples over a time interval of 90 seconds. Overall, the structure of angled layers allows for the control of material anisotropy and optimization of mechanical properties in various directions. This type of layering can absorb significant energy during failure due to the creation of a multiaxial stress state in the material, thereby increasing the fracture toughness of the composite. Woven fabrics, due to their intertwined fiber structure, provide high strength and dimensional stability. However, these types of composites exhibit lower fracture toughness compared to composites with angle plied layers, as the woven layers can be separated more easily.

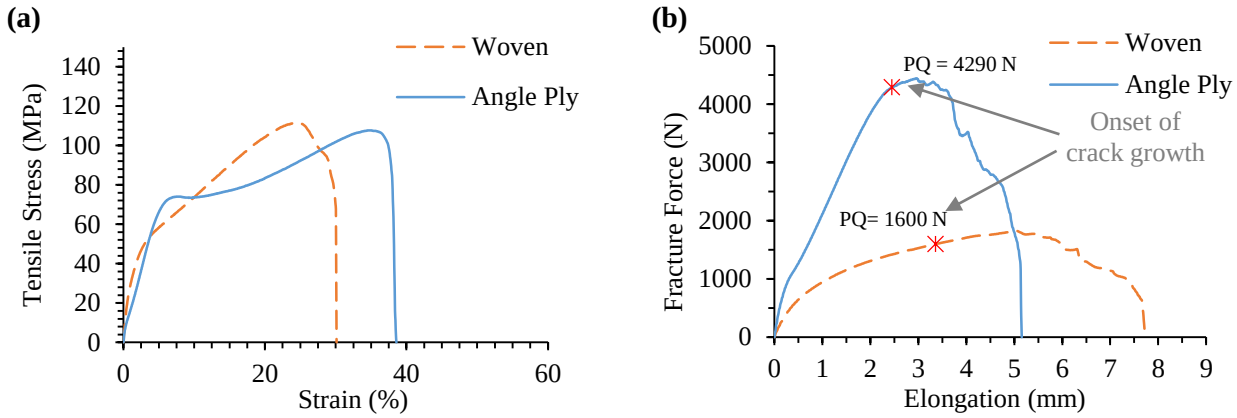

Fig. 5 Comparisons between a) stress-strain curves of the unnotched samples under tensile loads, b) force-displacement curves of the single-edge notched specimens under compact tension, in epoxy composites reinforced with different fibrous layers (woven fabric vs. angle plied layers) with ±45° fiber orientation

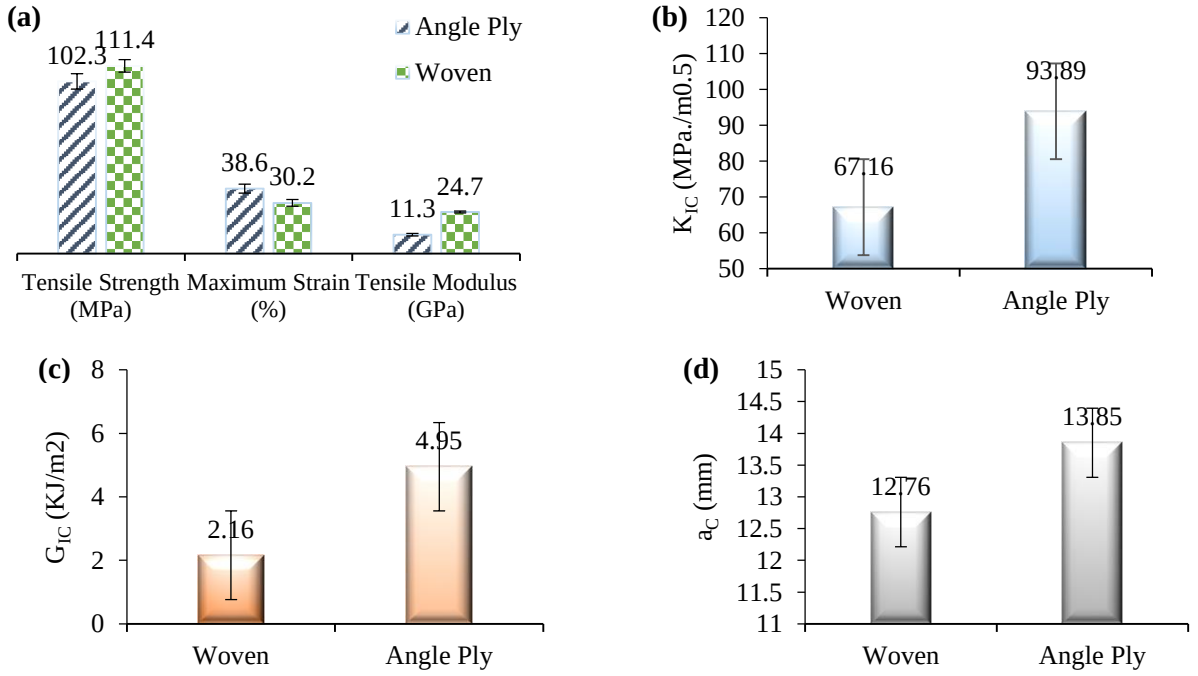

Fig. 6 Comparison of numerical values a) tensile properties in unnotched, and b) K_{IC}, c) G_{IC}, and d) a_C in single edge-notched epoxy composite samples reinforced with different fibrous layers, i.e., woven fabric vs. angled layers with ±45° fiber orientation under compact tension

Fig. 7 shows the crack growth in two different samples over a time interval of 90 seconds. Overall, the structure of angled layers allows for the control of material anisotropy and optimization of mechanical properties in various directions. This type of layering can absorb significant energy during failure due to the creation of a multiaxial stress state in the material, thereby increasing the fracture toughness of the composite. Woven fabrics, due to their intertwined fiber structure, provide high strength and dimensional stability. However, these types of composites exhibit lower fracture toughness compared to composites with angle plied layers, as the woven layers can be separated more easily.

The lower tensile strength and higher fracture toughness observed in the angle-plied composite can also be attributed to the higher void content. Therefore, from this aspect, tensile property degradation on one hand, and increased energy dissipation on the other, can be expected. However, the size and distribution of voids are also key parameters affecting these outcomes. Since the total void content in both specimens is very low, the dominant factor is still considered to be the difference in fiber layer configuration rather than the influence of void content.

Another important aspect is the difference in the thicknesses of the samples. It is well-known in fracture mechanics that apparent fracture toughness often decreases with increasing specimen thickness, due to the localized stress concentrations, nonuniform stress distribution, relatively small process zone, and three-dimensional crack propagation paths [22, 23]. In fiber reinforced polymer composites, however, thickness is not an independent factor. In fact, ply architecture inherently defines the thickness [24]. If thickness were the sole influencing factor, the thicker (angle-plied) specimen would be expected to show lower toughness. Instead, the angle-plied specimen exhibits higher toughness, which must then be attributed to its internal architecture (such as crack path tortuosity, fiber bridging, and constrained interlaminar delamination) rather than to thickness as an independent parameter. In angle plied architectures, the stress distribution forces cracks to follow more tortuous paths, allowing microscopic mechanisms and localized matrix deformations to absorb fracture energy more effectively. In contrast, in woven specimens, due to the interwoven structure of individual layers, the likelihood of delamination is higher. This phenomenon causes the initial cracks to propagate rapidly along the interlaminar surfaces, and consequently, despite their smaller thickness, the woven specimens exhibit lower fracture toughness.

3-4 Fractographic Analyses of the E-glass/epoxy Composites

SEM images illustrating the fracture features of the composite samples are presented in Fig. 8. Matrix grooves left by debonded fibers are obviously observed in the fractured surface of the composite prepared with woven layers, indicating delamination and interlayer separation. In contrast, in the specimen containing angle-plied players, the dominant failure mechanism is fiber pull-out from the matrix. Although localized layer separations are also observed in some regions, complete delamination has not occurred in angle plied sample.

The fractured surface of the matrix in the woven sample appears relatively smooth and flat, whereas microcracks and voids are evident in the matrix of the angle-plied counterpart. The presence of fibers also causes crack deflection and dissipates part of the fracture energy in changing the crack path, which well explains the higher critical energy release rate observed in the angle-plied composite. On the other hand, voids exert a complex influence on the mechanical behavior of the composite. As can be seen, small voids within the epoxy matrix has contributed in deflection of microcracks which can promote toughening mechanisms. In another hand, voids locally induce stress concentrations and promote the initiation of microcracks within the matrix under tensile stress. Therefore, these aspects can explain the tensile property degradation and increased energy dissipation behavior in angle-plied sample.

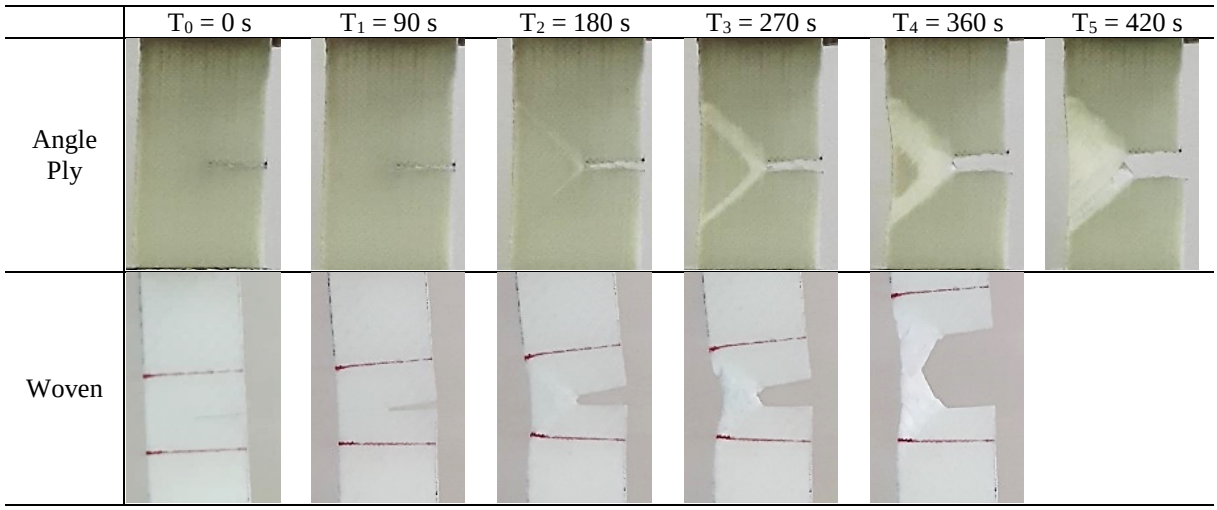

Fig. 7 Images showing the crack growth and propagation in two samples reinforced with angled layers and woven fabric

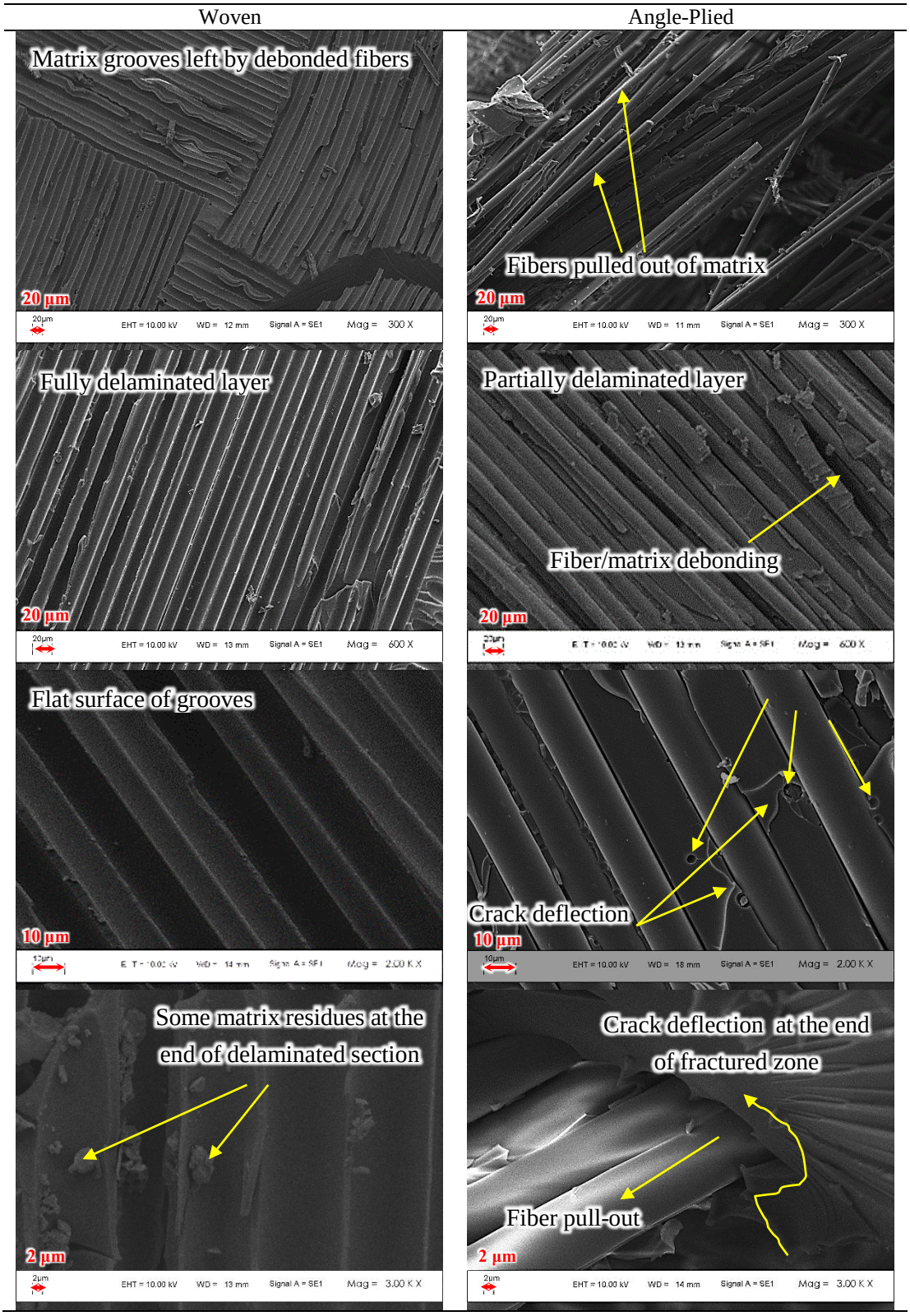

Fig. 8 SEM images of the fractured surfaces of the composite samples (woven vs. angle-plied) with different magnifications

4 CONCLUSIONS

This study investigated the tensile behavior and fracture parameters in two types of E-glass/epoxy composites, considering how the structure of fibrous layers affects the mechanical properties of the composite. The samples were produced in a four-layer configuration using the VIP technique. The first sample consisted of four layers of woven fabrics arranged at ±45º, while the second sample was made from four layers of angle plied layers oriented at ±45º. The results of this research are as follows:

- No significant difference was observed in fiber/matrix interfacial properties and fiber volume fraction in the two composite samples.
- The composite reinforced with woven fabrics exhibits high tensile strength and stiffness, but is more sensitive to crack growth.
- The composite reinforced with angle plied layers, despite being thicker, shows a 28.47% higher K_{IC} and a 56.36% higher G_{IC}, compared with woven counterpart.
- The lower thickness of the woven composite with the same areal density indicates a denser packing of fibers, which can enhance tensile performance but may lead to brittle fracture.
- Angle plied layers increase the thickness of the composite and provide less fiber cohesion, but allow for greater energy absorption and improved resistance to crack growth, compared with woven counterpart.

REFERENCES

[1] D. K. Rajak, D. D. Pagar, P. L. Menezes, and E. Linul, "Fiber-reinforced polymer composites: Manufacturing, properties, and applications," Polymers, vol. 11, no. 10, p. 1667, 2019.

[2] H. Jariwala, P. Jain, and V. Maisuriya, "Experimental and statistical analysis of strength of glass fiber reinforced polymer composite for different fiber architecture," Polymer Composites, vol. 42, no. 3, pp. 1407-1419, 2021.

[3] K. Chandra Shekar, B. Singaravel, S. Deva Prasad, N. Venkateshwarlu, and B. Srikanth, "Mode-I fracture toughness of glass/carbon fiber reinforced epoxy matrix polymer composite," Materials Today: Proceedings, vol. 41, pp. 833-837, 2021/01/01/ 2021, doi: https://doi.org/10.1016/j.matpr.2020.09.160.

[4] P. Morampudi, K. K. Namala, Y. K. Gajjela, M. Barath, and G. Prudhvi, "Review on glass fiber reinforced polymer composites," Materials Today: Proceedings, vol. 43, pp. 314-319, 2021.

[5] S. Y. Nayak et al., "Influence of fabric orientation and compression factor on the mechanical properties of 3D E-glass reinforced epoxy composites," Journal of Materials Research and Technology, vol. 9, no. 4, pp. 8517-8527, 2020/07/01/ 2020, doi: https://doi.org/10.1016/j.jmrt.2020.05.111.

[6] G. Raghavendra, P. P. Naidu, S. Ojha, B. Vasavi, M. Pachal, and S. K. Acharya, "Effect of bi-directional and multi-directional fibers on the mechanical properties of glass fiber-epoxy composites," Materials Research Express, vol. 6, no. 11, p. 115353, 2019/11/08 2019, doi: 10.1088/2053-1591/ab529a.

[7] V. Khatkar, A. G. S. Vijayalakshmi, R. N. Manjunath, S. Olhan, and B. K. Behera, "Experimental Investigation into the Mechanical Behavior of Textile Composites with Various Fiber Reinforcement Architectures," Mechanics of Composite Materials, vol. 56, no. 3, pp. 367-378, 2020/07/01 2020, doi: 10.1007/s11029-020-09888-0.

[8] K. Bilisik and G. Yolacan, "Experimental determination of bending behavior of multilayered and multidirectionally-stitched E-Glass fabric structures for composites," Textile Research Journal, vol. 82, no. 10, pp. 1038-1049, 2012, doi: 10.1177/0040517511420757.

[9] S. Risteska et al., "The Effect of Textile Structure Reinforcement on Polymer Composite Material Mechanical Behavior," Polymers, vol. 16, no. 24, doi: 10.3390/polym16243478.

[10] Y. Yang, Z. Miao, Y. Liu, H. Tu, and Y. Wei, "A comprehensive review of fiber-reinforced polymer-matrix composites under low-velocity impact," Mechanics of Advanced Materials and Structures, pp. 1-39, doi: 10.1080/15376494.2025.2458772.

[11] A. Siddique et al., "Mode I fracture toughness of fiber-reinforced polymer composites: A review," Journal of Industrial Textiles, vol. 50, no. 8, pp. 1165-1192, 2021, doi: 10.1177/1528083719858767.

[12] H. Dalfi, "Influence of Fibre Architectures on the Mechanical Properties and Damage Failures of Composite Laminates," Journal of Failure Analysis and Prevention, vol. 24, no. 4, pp. 1906-1915, 2024/08/01 2024, doi: 10.1007/s11668-024-01979-7.

[13] P. Sharma, H. S. Mali, and A. Dixit, "Mode-II interlaminar fracture toughness characterization of woven carbon–Kevlar interyarn hybrid textile composites," Iranian Polymer Journal, 2025/03/30 2025, doi: 10.1007/s13726-025-01485-z.

[14] H. Tewani, J. Cyvas, K. Perez, and P. Prabhakar, "Arχi-Textile composites: Role of weave architecture on mode-I fracture energy in woven composites," Composites Part A: Applied Science and Manufacturing, vol. 188, p. 108499, 2025/01/01/ 2025, doi: https://doi.org/10.1016/j.compositesa.2024.108499.

[15] S. A. M. Teroujeni, N. M. Khansari, and H. D. Hesar, "Mixed mode (I/II) fracture of Glass/PA6 thermoplastic composites based on hybrid distance and correlation-based multiple target tracking methods," Frontiers of Structural and Civil Engineering, vol. 19, no. 6, pp. 946-960, 2025/06/01 2025, doi: 10.1007/s11709-025-1189-0.

[16] H. Rahmani, S. H. M. Najafi, S. Saffarzadeh-Matin, and A. Ashori, "Mechanical properties of carbon fiber/epoxy composites: Effects of number of plies, fiber contents, and angle-ply layers," Polymer Engineering & Science, vol. 54, no. 11, pp. 2676-2682, 2014, doi: https://doi.org/10.1002/pen.23820.

[17] A. Alirezazadeh, S. M. Hejazi, A. Zadhoush, and S. Akbarzadeh, "Comparative Analysis of Textile Characteristics and Mechanical Properties of E-Glass Woven Fabrics in Epoxy Composites Under Cryogenic Conditions," Polymer Composites, vol. n/a, no. n/a, doi: https://doi.org/10.1002/pc.70551.

[18] P. Zinck, H. D. Wagner, L. Salmon, and J. F. Gerard, "Are microcomposites realistic models of the fibre/matrix interface? I. Micromechanical modelling," Polymer, vol. 42, no. 12, pp. 5401-5413, 2001/06/01/ 2001, doi: https://doi.org/10.1016/S0032-3861(00)00870-3.

[19] B. Miller, P. Muri, and L. Rebenfeld, "A microbond method for determination of the shear strength of a fiber/resin interface," Composites Science and Technology, vol. 28, no. 1, pp. 17-32, 1987/01/01/ 1987, doi: https://doi.org/10.1016/0266-3538(87)90059-5.

[20] S. Safi, A. Zadhoush, and M. Masoomi, "Evaluation of interfacial properties of the silane blend sized glass fiber–epoxy composite by the microdroplet test," Journal of Composite Materials, vol. 51, no. 11, pp. 1573-1581, 2017, doi: 10.1177/0021998316661620.

[21] A. Inernational, "Standard test methods for plane-strain fracture toughness and strain energy release rate of plastic materials," ASTM D5045-99, 2007.

[22] F. Minami, M. Toyoda, and K. Satoh, "A probabilistic analysis on thickness effect in fracture toughness," Engineering Fracture Mechanics, vol. 26, no. 3, pp. 433-444, 1987/01/01/ 1987, doi: https://doi.org/10.1016/0013-7944(87)90024-5.

[23] X. Xu, A. Paul, and M. R. Wisnom, "Thickness effect on Mode I trans-laminar fracture toughness of quasi-isotropic carbon/epoxy laminates," Composite Structures, vol. 210, pp. 145-151, 2019/02/15/ 2019, doi: https://doi.org/10.1016/j.compstruct.2018.11.045.

[24] R. F. Teixeira, S. T. Pinho, and P. Robinson, "Thickness-dependence of the translaminar fracture toughness: Experimental study using thin-ply composites," Composites Part A: Applied Science and Manufacturing, vol. 90, pp. 33-44, 2016/11/01/ 2016, doi: https://doi.org/10.1016/j.compositesa.2016.05.031.